Water erosion as a fractal growth process

Hajime Inaoka
Department of Earth Sciences, Kobe University, Kobe 657, Japan

Hideki Takayasu
Department of Earth Sciences, Kobe University, Kobe 657, Japan
and The Graduate School of Science and Technology, Kobe University, Kobe 657, Japan

(Received 21 September 1992)

The time evolution of river patterns and earth's relief is simulated on lattice by modeling the process of water erosion. Starting from a randomly perturbed surface, the river pattern and earth's relief develop simultaneously. The river pattern becomes stationary after all lakes have vanished. In the stationary state the river pattern shows some fractal properties such as a power-law size distribution of the drainage basin area and Horton's laws. The fractalities are shown to be not exactly self-similar but self-affine. A mean-field theory for the river pattern is discussed.

PACS number(s): 64.60.Ht, 92.40.Gc, 05.70.Ln, 68.45.Ws

I. INTRODUCTION

It is now widely known that there exist many fractal geometries in nature [1–4]. Landscapes such as coastlines and river patterns are familiar examples to us, and their fractalities are supported by numerical analyses of the real topographical data [1,5,6].

The fractality of landscapes was pointed out by Mandelbrot with the proposal of the concept of fractals [1]. He also proposed a model which creates the fractal surfaces, so-called Brownian surfaces, and the product is regarded as a model of earth's relief [1]. But the processes of the landform creation in his model are far removed from real processes of landform evolution, so the model does not describe what creates the fractality on the landform nor how the fractal landform is evolved. The fact that the fractals on the earth's relief exist over such an extensive region implies that the fractals are probably created by a kind of fractal growth process from nonfractal surfaces.

In recent years, knowledge about fractal growth has been rapidly accumulating. The model of fractal growth that has received the most attention may be that of Laplacian fractals, such as the diffusion-limited-aggregation model [7] (DLA) or the dielectric-breakdown model [8] (DBM). In the growth of Laplacian fractals, it is crucial that the local growth of the cluster is governed by the total shape of the cluster. More concretely, the shape of the cluster determines the Laplacian field surrounding the cluster, and the local growth velocity or probability of the cluster is proportional to the gradient of the Laplacian field at the surface of the growth point. Thus, the Laplacian field surrounding the cluster has the role of the "medium" which transmits the information about surrounding structures of the cluster to a local growth point. With regard to the landform evolution process from the point of view of a fractal growth phenomenon, it is an important problem whether there exists such a "medium" or not.

There are many factors causing the changes of landscapes—for example, tectonic movement, sedimentation, water erosion, weathering, and so on. Among those factors, we give consideration here to the water-erosion process.

In the water-erosion process, the local intensity of erosion depends upon the area of the drainage basin through the water on the surface. That is, if we neglect the effect of underground water and evaporation, the quantity of the water is determined by the amount of rainfall which is gathered by the drainage basin, and the local erosion speed is controlled by the quantity of water flowing on the point.

This situation of landform evolution by water erosion is similar to that of Laplacian fractals in the sense that the global structure in the system governs the local growth. So, the water on the earth's relief is expected to perform the role of a "medium" which conveys the information about the drainage-basin area and governs the local erosion intensity.

For many years, the formation of landscapes and the geometrical structure of river patterns have been studied. With regard to river patterns, various stochastic models have been proposed to reproduce the statistical properties of real river patterns, such as Horton's laws [9]. The most famous examples of them may be Scheidegger's river model [10] and the self-avoiding random-walk model originally proposed by Leopold and Langbein [11], which is recently investigated in more detail by Meakin, Feder, and Jøssang [12]. Scheidegger's river model is the model for the river pattern on a slope of a two-dimensional triangular lattice. The river pattern is obtained by assigning two kinds of flow vectors, right down and left down, randomly to each lattice point. As shown in this procedure, the resulting river patterns are static and not based on erosional landform evolution, i.e., they neglect the water on the earth's relief. Geomorphologists have proposed some landform evolution models including the effect of water erosion. The models proposed by

Roth, Siccardi, and Rosso [13] and Willgoose, Bras, and Rodriguez-Iturbe [14] are the recent examples. In particular, the evolution rule of the latter is an elaborate one based on the detailed geomorphological studies. However, such a detailed algorithm is not suitable for numerical calculation because the system size is limited by CPU time. The system size is essential when we observe fractal properties of the model; therefore, the model should be as simple as possible. Moreover, if the fact that the local growth is influenced by the surrounding structure is essential for the fractal growth, the mechanisms of the local growth can be drastically simplified. Kramer and Marder proposed a kind of minimal model of erosion process [15]. But, as we mention in Sec. II, the model includes the stochastic water flow process. To treat the water-erosion process as a fractal growth process, the water-flow process which connects the local erosion and surrounding structures is preferably deterministic.

Recently, the authors have proposed a kind of minimal model of erosion and performed numerical simulations of landform evolution in relatively large systems (512×512) [16]. It is found that the system reaches a fractal steady state which is created automatically without any tuning parameters, and in this sense, the model can be regarded as a kind of self-organized criticality [17]. This paper is devoted to an explanation of the details of our erosion model.

We describe the model and show numerical results in Secs. II and III. Statistical properties of the steady-state river pattern are analyzed in Sec. IV where we confirm a power-law drainage area distribution and Horton's laws. We introduce a mean-field theory in Sec. V and give theoretical supports for these results. Section VI is devoted to a discussion on the fractal dimensions of river patterns and landforms. We show that river patterns seem to posses self-affinity rather than self-similarity. A short summary is given in Sec. VII.

II. DESCRIPTION OF THE MODEL

We model the water-erosion process only by the water from rainfall, that is, we neglect the effect of underground water, infiltration, evaporation, and weathering. Therefore, the quantity of water on the land which is given by the sum of the amount of rainfall, is conserved in the water-flow process. We assume the situation that rain is falling on the land uniformly and constantly. The land we use in the model has no geographical structure and crustal movement, that is, it is uniform and static. We also assume that the sand produced by erosion is smoothly washed away by water flow, so that the sedimentation of sand is neglected. Because of this assumption, the height of the land at each point decreases monotonically and never increases.

Under these conditions, we model the processes such as rainfall, water flow, water erosion, and formation and vanishment of lakes. The rules used in our system are local and deterministic, so the randomness comes only from the initial condition.

Our model is defined on a two-dimensional triangular lattice. Every site (x,y) has three variables: $h(x,y)$, the height of the land; $s(x,y)$, the water-flow intensity; and $w(x,y)$, the thickness of water accumulation. The height of the water surface, $h_w(x,y)$, is defined as

$$h_w(x,y)\equiv h(x,y)+w(x,y)\ .$$

Note that the water-flow intensity does not contribute to the height of the water surface since it is assumed to have no thickness. The thickness of water accumulation is introduced to realize the formation and vanishment of lakes, and does not relate to the water-erosion process. A site for which $w(x,y)$ is not zero is called a "lake" site.

For a given landform $h(x,y)$, the time evolution of the system is performed by repeating the following procedures. The $s(x,y)$ and $w(x,y)$ on the surface are given initially.

(1) Determination of water-flow direction. For every site (x,y), we find the site (x',y') which has the lowest height of water surface in the six nearest neighbors. When $h_w(x,y)>h_w(x',y')$, the water-flow direction of the site (x,y) is determined as the direction to the site (x',y'). However, if $h_w(x,y)\le h_w(x',y')$, it becomes unnatural to flow out $s(x,y)$ to the site (x',y'). In this case, $w(x,y)$ is renewed by

$$w(x,y)\equiv h_w(x',y')-h(x,y)+\epsilon$$

to raise the water surface, where ϵ is a very small positive number. On the other hand, it is quite natural to assume that $w(x,y)$ becomes zero when $h(x,y)>h_w(x',y')$. So we make $w(x,y)$ zero at such a site. We can draw a global water-flow pattern which we call a river pattern when the water-flow directions for all sites are determined (Fig. 1).

(2) Water erosion. By the effect of water erosion, $h(x,y)$ is decreased by

$$\delta h(x,y)=F(J(x,y))\{h_w(x,y)-h_w(x',y')\}\ ,$$

where $J(x,y)$ denotes the water power which is defined as

$$J(x,y)\equiv s(x,y)\{h_w(x,y)-h_w(x',y')\}\ .$$

The function F is a positive monotonically increasing function which satisfies $F(0)=0$ and $\lim_{J\to\infty}F(J)<1$. In this paper we use $F(J)=CJ^a/(1+J^a)$, where C and a are positive constants.

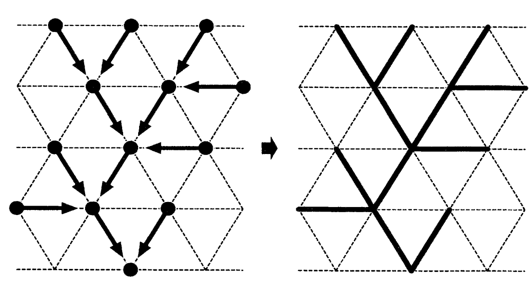

FIG. 1. The formation of river pattern. The arrows in the left part show the flow directions.

(3) Water flow and rainfall. The $s(x,y)$ is moved to the site (x',y'). The new $s(x,y)$ is determined as the sum of s from nearest neighbors and a constant s_0. This s_0 corresponds to the water from rainfall.

(4) Repeat the above procedures. Procedures 1, 2, and 3 make one time step. These procedures are done on all sites at the same time.

Procedure 1 is based on the intuitively natural fact that the water on the surface flows toward the lowest place. The procedures about formation and vanishment of lakes may look rather artificial, but they have a fairly important role. If there is a global basin area in the system, the lake water fills the area and erodes the lowest place of the lake edge selectively and intensively, and from there, the erosional landscapes evolve upward. Thus the lake water has the role of transmitting the information about the location of the drainage outlet or the direction that the water on the surface should flow to. To realize the above situation of lake formation, we can take another approach by introducing the water-flow intensity which has thickness. But if we take this model, we have to abandon the simultaneousness of the procedures to suppress the vibration of water on the surface. Kramer and Marder resolved the vibration by limiting the operating site to one which is randomly chosen from the system [15], but it is rather unphysical and unreasonable from the point of view of the propagation of information.

III. TIME EVOLUTION OF THE SYSTEM

We use the initial landform such as

$$h(x,y)=2000.0+\{\text{uniform random fluctuation ranging } [0,0.1)\} ,$$

namely, it has a flat surface perturbed by very slight white noise. In the initial condition, there is no water on the land, i.e., $s(x,y)=0$ and $w(x,y)=0$ for every site. The parameters for $F(J)$ used in this paper are $C=0.5$, $s_0=10^{-5}$, and $a=0.5$, 0.8, 1.0, 1.2, and 1.5. The left- and right-side edges of the system are connected by the periodic boundary condition. A high wall is built on the top-side edge, while the height of the bottom-side edge is zero and fixed, so all of the water in the system flows out from the bottom-side edge. We use a system of size 512×512 for the numerical results shown in this paper. We mainly discuss the results from the case $a=1$ in the text, and the results from the cases of other a and Scheidegger's river model for a comparison are collectively shown in Table I.

Figure 2 shows an example of time evolution of a landform in the case $a=1$. As we can see from this series of figures, the valleys grow from the bottom-side edge to the top-side edge. The behavior of the erosion function $F(J)$ for small J depends on the value of a. It is interesting to show the difference in landscapes for different a. Figure 3 shows a landform evolved in the case $a=1.5$. As can be seen by comparing these figures, the valleys look narrower and steeper for large a.

We plot the number density of lake sites and unstable sites which change the flow direction in one time step in Fig. 4. Initially, almost all sites are covered by lakes, and the number of lake sites decreases monotonically with the evolution of valleys, as seen in Fig. 2. About the time that valleys spread over the whole surface, the number of lake sites becomes zero. In this stage, the number of unstable flows also becomes zero, namely, it becomes a kind of steady state where all sites in the system do not change their flow directions. This steady state is very stable, so once the system reaches this steady state, the river pattern on the surface never changes while the erosion process of land progresses. In the following, we use the term steady state for a system which has had no lake sites and no unstable sites in the past 50 time steps.

Figure 4 shows the case $a=1$. In the case of other a,

TABLE I. The numerical results of the simulation of size 512×512 for different values of parameter a. The results for Scheidegger's river model are also shown for comparison. The values in the parentheses are the theoretical results [23].

Parameter a	0.5	0.8	1.0	1.2	1.5	Scheidegger's model	Error range
Power-law exponent of drainage-basin area distribution, β	0.43	0.42	0.42	0.41	0.40	0.36 ($\frac{1}{3}$)	0.01
Bifurcation ratio R_B	5.4	5.3	5.3	5.2	5.1	4.7	0.4
Stream-length ratio R_L	2.7	2.7	2.7	2.7	2.7	3.0	0.1
Fractal dimension of the river patterns from Horton's ratios D_s	1.69	1.67	1.66	1.66	1.65	1.40	
Fractal dimension of the river patterns from β, D_β	1.75	1.72	1.72	1.70	1.69	1.58 ($\frac{3}{2}$)	
Hack's exponent α	0.60	0.62	0.62	0.63	0.64	0.68 ($\frac{2}{3}$)	0.02

similar results are obtained, that is, the systems also reach steady states where the river patterns are frozen. However, they still take more time steps for larger a. An example of a steady-state river pattern is displayed in Fig. 5. In the following sections, we focus our attention mainly on this steady-state river pattern.

In our model, the randomness of the resulting landform comes only from the initial condition, so we check the sensitivity to the initial landform of our model. We prepare two identical initial landforms $h_1(x,y)$ and $h_2(x,y)$, and put a noise $(=0.1)$ on a randomly chosen site of $h_2(x,y)$. These two landforms are evolved and the Humming distance

$$d_H \equiv \sum_{x,y} |h_2(x,y) - h_1(x,y)| \ ,$$

is calculated for every time step. Figure 6 shows a result of the case $a=1$ in log-log scale. The points are on a straight line ranging from 200 to 1000 time steps, while they look irregular at the beginning. This result shows that the Humming distance d_H expands as $d_H \propto t^{2.6}$, namely, errors do not grow exponentially in our model, indicating that the system is at the edge of chaos as in the model of self-organized criticality [17].

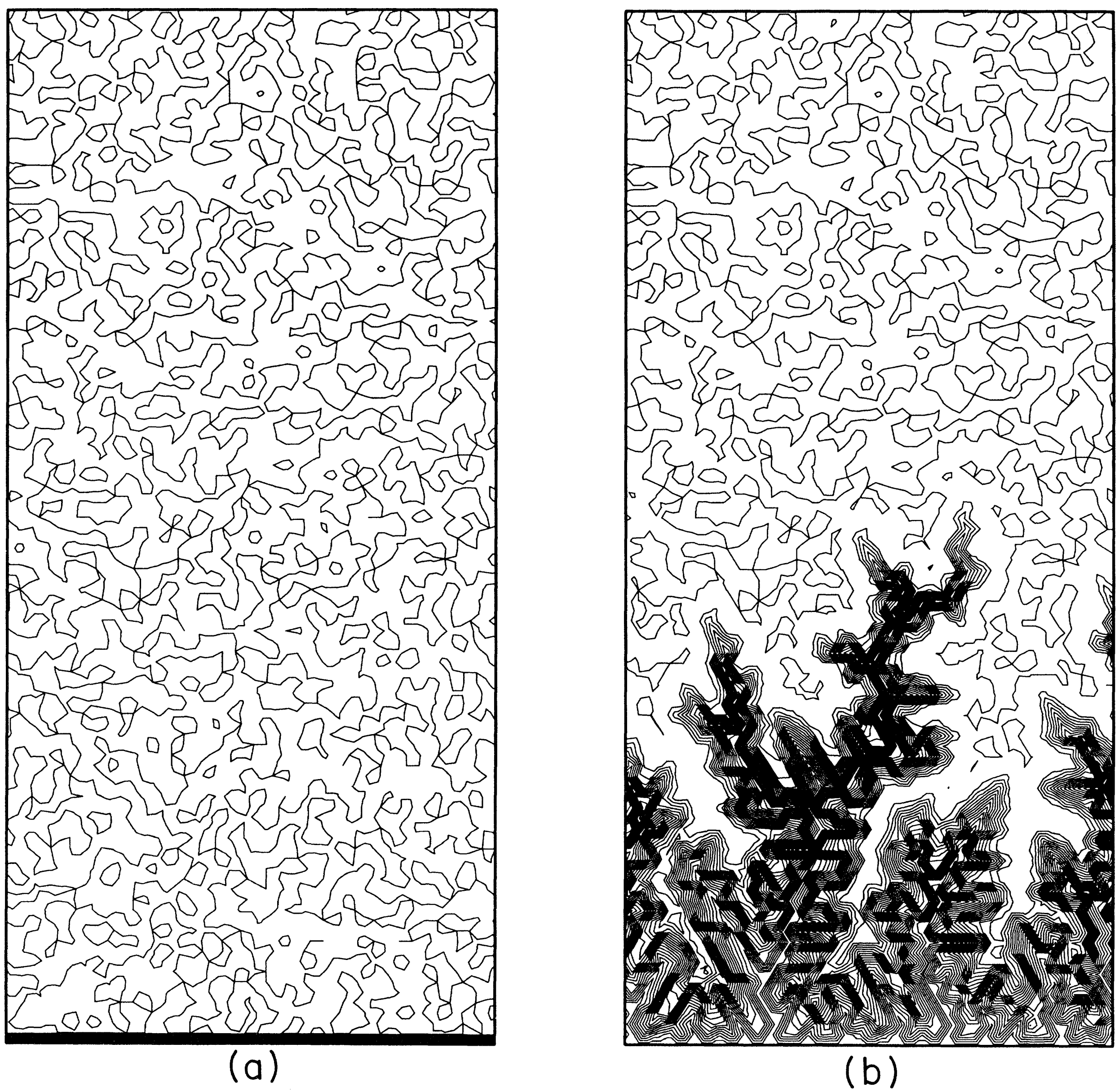

FIG. 2. A series of contour map of landform evolution. A part (40×100) of the system of size 100×100 is illustrated. (a) Initial condition. (b) At 300 time steps. (c) At 600 time steps. (d) At 1500 time steps.

IV. STATISTICS OF STEADY-STATE RIVER PATTERNS

In this section we study some statistical properties of steady-state river patterns of our model.

A. Drainage-basin area distribution

The fractal branch geometries can be characterized by the exponent of the power-law distribution of branch size [18]. In our model, the branch size corresponds to the drainage-basin area of the stream. Here, the drainage basin area at the site (x,y), $n(x,y)$ means the number of sites which are upstream of the site (x,y), and it is equal to $s(x,y)/s_0$ on the steady-state river pattern.

We plot the cumulative distribution of drainage-basin area in log-log scale in Fig. 7. In the figure, $P(\geq n)$ means the probability that a certain randomly chosen site has a drainage-basin area value larger than or equal to n. The points are on a straight line in the range from $s=10^1$ to 10^3; this result shows that the cumulative distribution of basin size follows a power law $P(\geq n) \propto n^{-\beta}$, $\beta=0.42$. For $n > 10^3$, the points deviate from the line because of the finite-size effect of the system. To estimate the exponent of distribution in the infinite-size system, we plot the exponents of the basin size distribution estimated from systems of various sizes (Fig. 8). The points are roughly on a line and the exponent of the cumulative basin size distribution in the infinite-size system is estimated to converge at $\beta=0.42$.

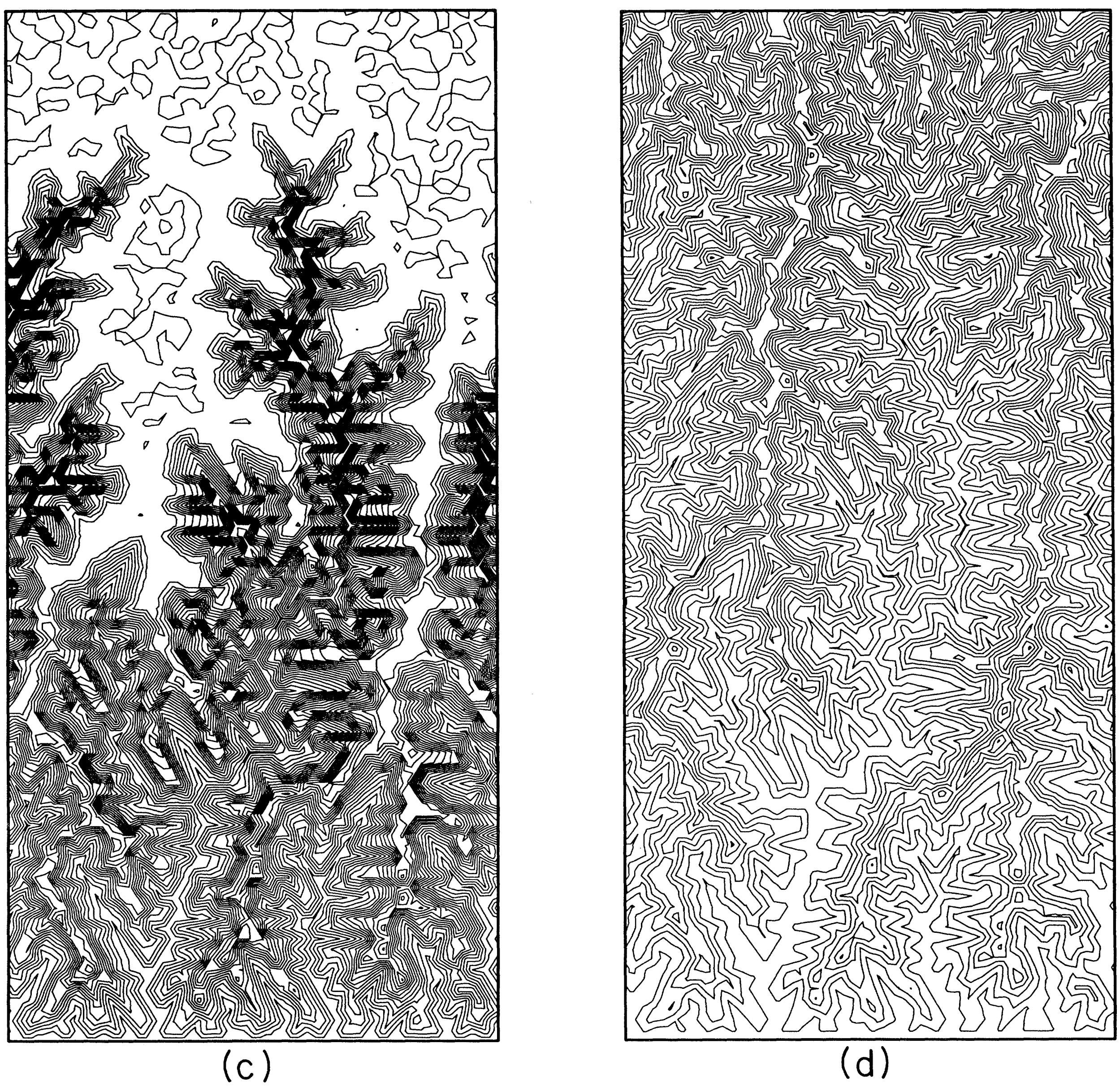

FIG. 2. (*Continued*).

B. Horton's laws

Real river patterns are known to satisfy Horton's laws [9]. In this section we check the validity of these laws for the river pattern from our model. At first, we must determine the stream order on the river pattern.

Horton's stream order is defined as follows: The order of all up ends of the stream are 1, and we trace streams downward from these up ends. At a confluence of inflowing streams, the stream orders of these inflowing streams are checked, and among them, we choose the highest value of stream order, $\omega_{\max}$. The order of outflowing streams is given by this $\omega_{\max}$. If the orders of the two streams are both $\omega_{\max}$, the order of the outflowing stream is defined as $\omega_{\max}+1$. We also relabel the order of the longer inflowing stream as $\omega_{\max}$. Because of this additional procedure, we can easily find the main stream of the stream network (see Fig. 9). The tracing is continued until it reaches the mouth of the river.

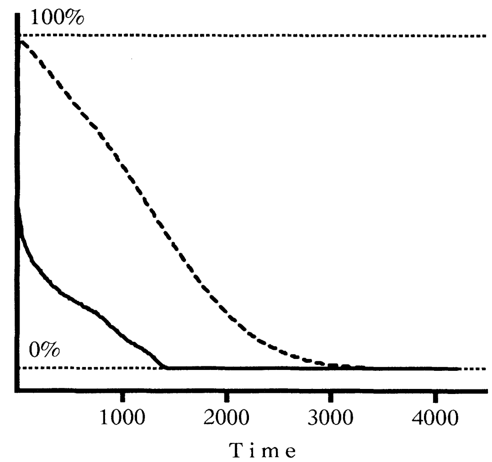

FIG. 4. The number density of lake sites (dashed line) and unstable sites (bold line). The number is shown as a percentage.

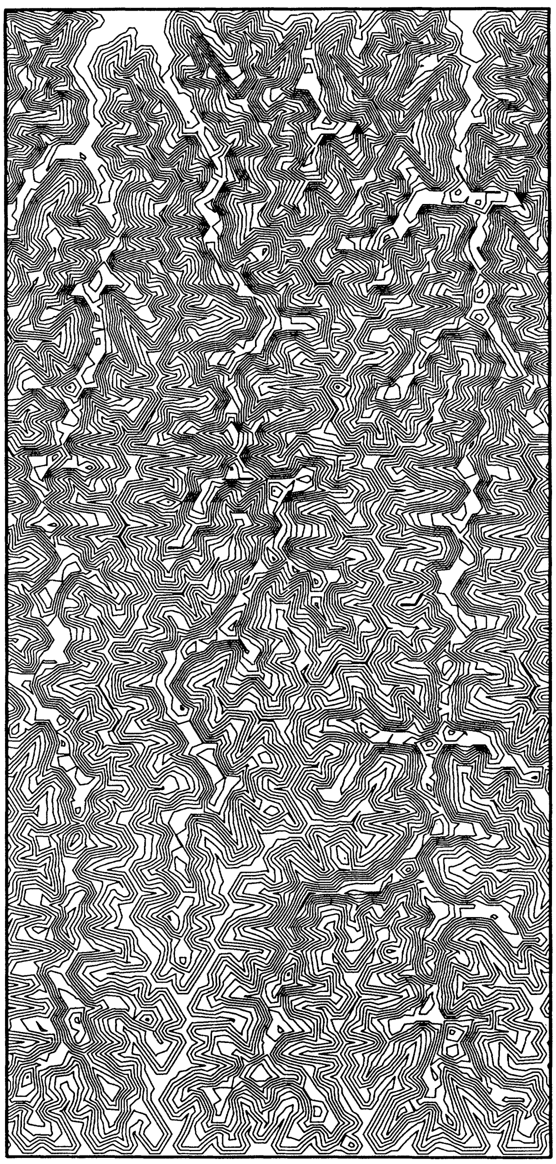

FIG. 3. A contour map of the landform for the case $a=1.5$. Initial condition, system size, and the part presented are same as in Fig. 2. It takes 6000 time steps.

There is another definition of stream order—Strahler's stream order. The difference between these two stream orders is that Strahler's stream order does not determine the main stream. That is, in the above procedure, at a confluence of streams when more than two inflowing streams have the maximum order $\omega_{\max}$, we only fix the stream order of outflowing stream as $\omega_{\max}+1$. The difference between these two stream orders is illustrated in Fig. 9.

Using Horton's stream order, we count the number of ω order streams, N_ω, and measure the averaged length of ω order streams, L_ω. Horton's laws insist that the ratios

$$N_\omega/N_{\omega+1}=R_B,\quad L_{\omega+1}/L_\omega=R_L$$

are independent of ω. The constants R_B and R_L are called the bifurcation ratio and the stream-length ratio, respectively. These laws are known to be also valid in the case when Strahler's stream order is used [19,20].

Using Horton's stream order, we plot N_ω and L_ω in semilog scale in Fig. 10. The points are clearly on straight lines except the points for the highest order. The highest-order stream seems to be influenced by the finiteness of the system. Taking the finite-size effect into account, we estimate $R_B=5.3$ and $R_L=2.7$ in the case $a=1$. These results seem to have comparatively large errors because we can use only seven or eight points to estimate these ratios (see Fig. 10).

The empirical ranges of these ratios estimated from real systems are $R_B=2-6$ and $R_L=1.5-3.5$ [6]. The results of our model are in these ranges.

V. MEAN-FIELD THEORY

Here we present a theoretical approach for the statistical properties mentioned in Sec. IV.

A. Drainage-basin area distribution

We choose one site at random from the steady-state river pattern. Let p_k be the probability that the number of streams which flow into the chosen site is k, and n_i $(i=1,2,\ldots,k)$ the drainage-basin area of the site which has an inflowing stream to the chosen site. Since every site in the steady-state system has one outflowing, the expectation of the number of streams which flow into the chosen site must be 1, so p_k satisfies the following two equations:

$$\sum_k p_k = 1 , \tag{1}$$

$$\sum_k k p_k = 1 . \tag{2}$$

Note that k takes only 0, 1, 2, and 3 in the steady-state river pattern on a triangular lattice. The drainage-basin area for a site n is the sum of n_i and the number of the site itself $=1$, that is,

$$n = n_1 + n_2 + \cdots + n_k + 1 . \tag{3}$$

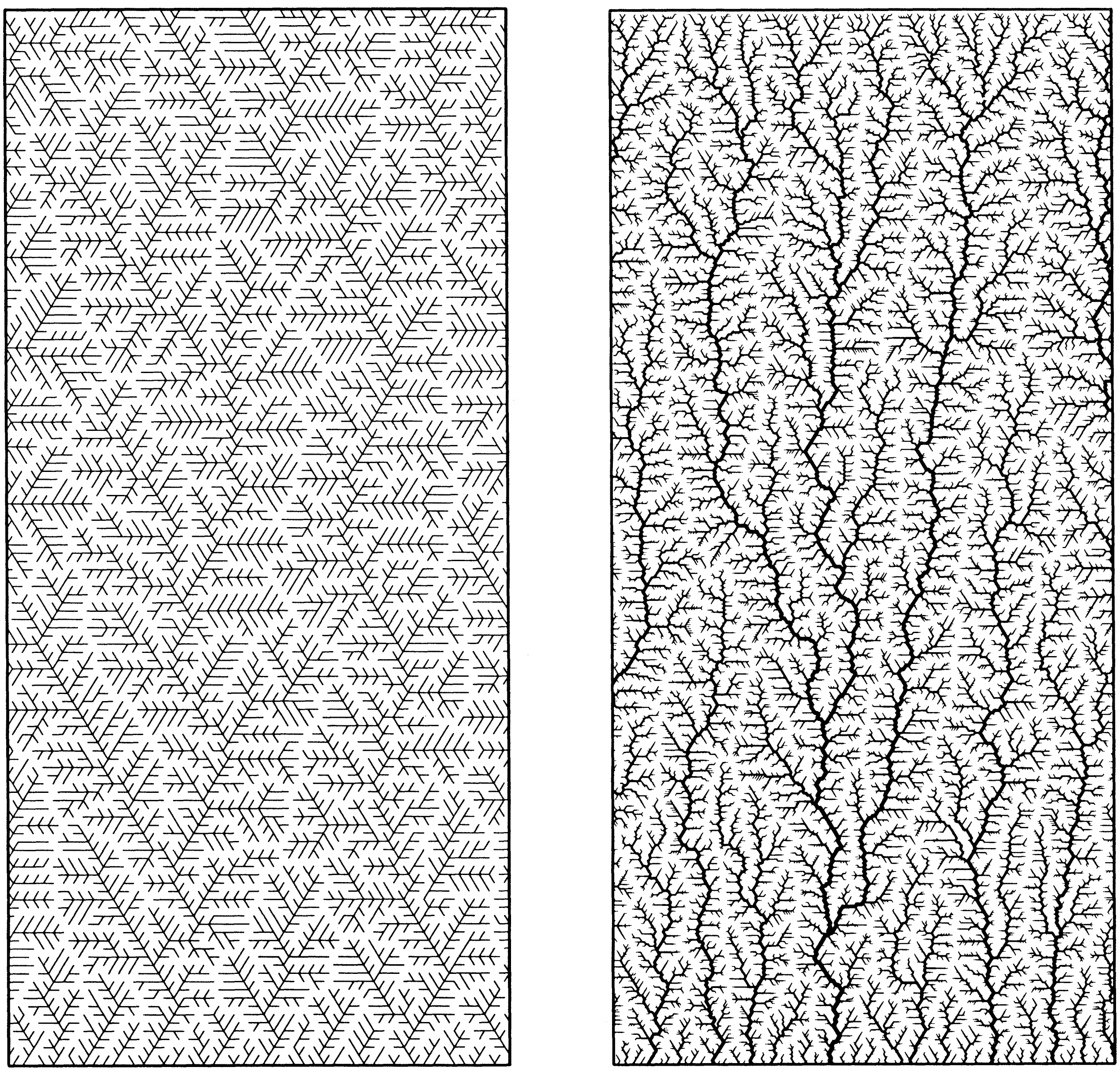

(a) (b)

FIG. 5. An example of a steady-state river pattern from the system of size 512×512: (a) An enlargement of the system. The part of size 50×128 is illustrated. (b) The part of size 200×512. The thickness of the pattern is proportional to the logarithm of the water-flow intensity.

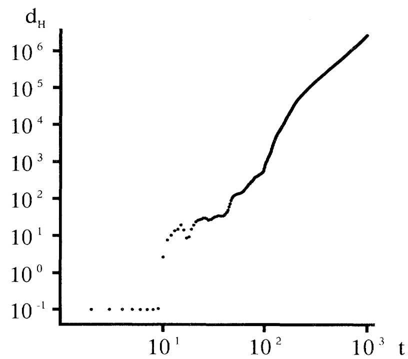

FIG. 6. The time evolution of the Humming distance d_H of the case $a=1$ in log-log scale. The straight part of the line ranging from 200 to 1000 time steps shows that the errors grow as $d_H \propto t^{2.6}$.

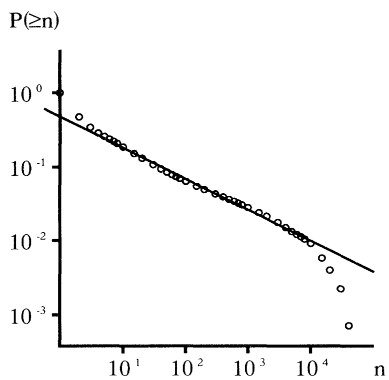

FIG. 7. Cumulative distribution of the drainage-basin area $P(\geq n)$ of the case $a=1$ in log-log scale. The line shows a power law as $P(\geq n) \propto n^{-0.42}$.

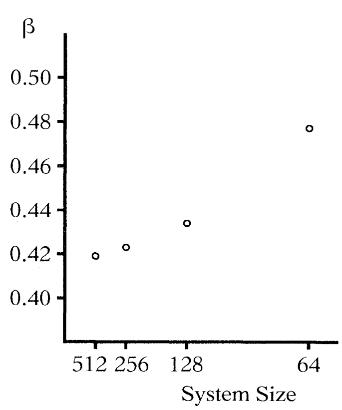

FIG. 8. The finite-size effect of exponent β, $P(\geq n) \propto n^{-\beta}$, from the model of the case $a=1$. The system size is shown by its inverse.

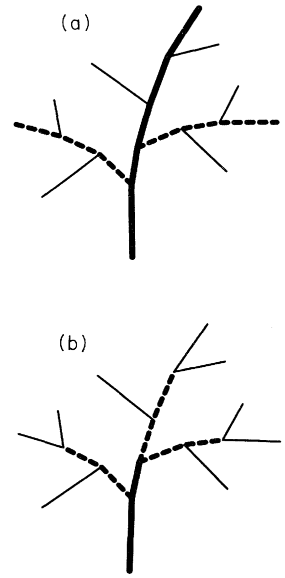

FIG. 9. The stream orders determined in two different ways for the same stream network: (a) Horton's stream order and (b) Strahler's stream order. The fine lines, dashed lines, and bold line show first-, second-, and third-order streams, respectively.

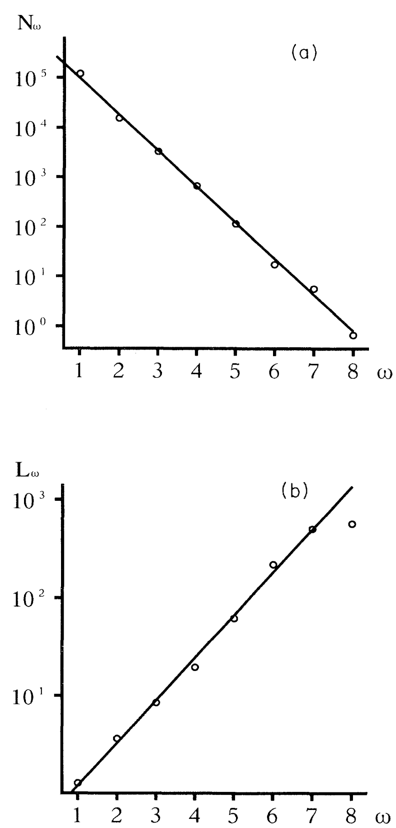

FIG. 10. Relations of stream order ω and (a) the number of stream branches N_ω and (b) the averaged stream length L_ω in semilog scale. The river pattern from the case $a=1$ is used.

By treating the nearest-neighbor sites as mean-field sites, the distribution of $n, P(n)$ follows the equation

$$P(n)=\sum_k p_k \sum_{n_1+n_2+\cdots+n_k=n-1} P(n_1)P(n_2)\cdots P(n_k) \ . \tag{4}$$

Instead of treating the distribution itself, we introduce the characteristic function $Z(\rho)$, the Laplace transform of $P(n)$, which is defined as

$$Z(\rho)\equiv \sum_{n=1}^{\infty} e^{-\rho n}P(n) \ . \tag{5}$$

We obtain the equation for $Z(\rho)$ by transforming both sides of Eq. (4):

$$Z(\rho)=e^{-\rho}\sum_k p_k Z(\rho)^k \ . \tag{6}$$

The asymptotic behavior of $P(n)$ for $n\rightarrow\infty$ corresponds to that of $Z(\rho)$ for $\rho\rightarrow 0$. To explore this behavior, we expand $Z(\rho)$ around $\rho=0$. By definition $Z(\rho)=1$; we can put $Z(\rho)$ as

$$Z(\rho)\equiv 1+\tilde{Z}(\rho), \quad |\tilde{Z}(\rho)| \ll 1 \ . \tag{7}$$

Substituting Eq. (7) into Eq. (6) and using Eqs. (1) and (2), we find that

$$\tilde{Z}(\rho)\propto \rho^{1/2} \ , \tag{8}$$

so $Z(\rho)$ is obtained as

$$Z(\rho)=1+\text{const}\times\rho^{1/2}+\cdots \ . \tag{9}$$

Equation (9) indicates that the distribution of $n, P(n)$ is proportional to $n^{-3/2}$ for large n. The cumulative distribution of n becomes

$$P(\geq n)\propto n^{-1/2} \ , \tag{10}$$

which shows that the mean-field exponent β is 0.5. It is easy to show that if we omit the steady-state condition, Eq. (2), then the distribution of n always has an exponential decay. That is, the steady-state condition that every site has one outflowing stream automatically makes the system critical.

B. Horton's laws

Our first task is to calculate the site-number ratio. Let S_ω be the number of sites which belong to the ω order stream. We use Strahler's stream order here. The site-number ratio R_S is defined as $R_S\equiv S_\omega/S_{\omega+1}$. Using the total site number of the system $S=\sum_\omega S_\omega$ and S_ω, the probability W_ω that a chosen site in the system belongs to a stream of order ω is given by

$$W_\omega\equiv S_\omega/S \ . \tag{11}$$

Here we consider the situation that the maximum number of inflowing streams at a confluence is 2, while it is 3 in our simulation. In the case that the number of inflowing streams is 2, the stream order of outflowing stream ω is determined as follows in terms of the stream orders of inflowing streams ω_1 and ω_2:

$$\omega=\begin{cases}\max\{\omega_1,\omega_2\} & (\omega_1\neq\omega_2) \\ \omega_1+1 & (\omega_1=\omega_2)\end{cases} \ . \tag{12}$$

Also taking into account the cases of $k=0$ and 1, we have five cases of ω, the order of outflowing streams of the chosen site, with probabilities given as follows:

$k=0,\ \omega=1$ with probability p_0

$k=1,\ \omega=\omega_1$ with probability $p_1 W_{\omega_1}$

$$k=2,\begin{cases}\omega=\omega_1 \text{ with probability } p_2 W_{\omega_1}\sum_{j=1}^{\omega_1-1} W_j \\ \omega=\omega_2 \text{ with probability } p_2 W_{\omega_2}\sum_{j=1}^{\omega_2-1} W_j \\ \omega=\omega_1+1 \text{ with probability } p_2 W_{\omega_1}^2 \ .\end{cases}$$

Thus we obtain the equations for W_ω as

$$W_1=p_0+p_1W_1 \ , \tag{13}$$

$$W_\omega=p_1W_\omega+2p_2W_\omega\sum_{j=1}^{\omega-1}W_j+p_2W_{\omega-1}^2 \ . \tag{14}$$

Using Eqs. (1) and (2) of the case $k=0$, 1, and 2, we find $W_1=\frac{1}{2}$ and $W_\omega=2^{-\omega}$. So the site-number ratio R_S is independent of ω and is estimated as

$$R_S=\frac{S_\omega}{S_{\omega+1}}=\frac{W_\omega}{W_{\omega+1}}=2 \ . \tag{15}$$

Next we consider the averaged stream length of an ω order stream. The probability that a stream starting with order ω remains to be of the same order in l sites is given as

$$\left[p_1+p_2\sum_{j=1}^{\omega-1}W_j\right]^{l-1} p_2\left[1-\sum_{j=1}^{\omega-1}W_j\right](p_2W_{\omega-1}^2)^{-1} \ . \tag{16}$$

The expectation of l, L_ω is then calculated as

$$\begin{aligned}L_\omega&=\sum_{l=1}^{\infty} l\left[p_1+p_2\sum_{j=1}^{\omega-1}W_j\right]^{l-1} p_2\left[1-\sum_{j=1}^{\omega-1}W_j\right](p_2W_{\omega-1}^2)^{-1} \\ &=\sum_{l=1}^{\infty} l\{p_1+p_2(1-2^{1-\omega})\}^{l-1}\{1-(1-2^{1-\omega})\}2^{2(\omega-1)}=\{p_2(1+2^{1-\omega})\}^{-2}2^{\omega-1} \ .\end{aligned} \tag{17}$$

Therefore, we get the stream-length ratio R_L for large ω as

$$R_L = \lim_{\omega\to\infty} \frac{L_{\omega+1}}{L_\omega} = 2 . \tag{18}$$

The number of streams of order ω in the system is given by $N_\omega = S_\omega / L_\omega$, so the bifurcation ratio $R_B = N_\omega / N_{\omega+1}$ is calculated from R_S and R_L as

$$\frac{N_\omega}{N_{\omega+1}} = \frac{S_\omega}{S_{\omega+1}} \frac{L_{\omega+1}}{L_\omega} = R_S R_L = 4 . \tag{19}$$

Summarizing these results, the mean-field Horton's ratios are $R_B = 4$ and $R_L = 2$.

VI. ABOUT FRACTAL DIMENSIONS

The fractal structures are usually characterized by fractal dimensions. As shown in the above sections, the river patterns in our model have the fractal property described by the power-law distribution of the drainage-basin area. In addition, there is another fractal geometry in the product of our model—the earth's surface. In this section we discuss these fractal properties in terms of fractal dimensions.

A. For the river patterns

Intuitively, Horton's laws can be recognized as representing the fractality of river networks. La Barbera and Rosso propose an equation which relates the fractal dimension of a river network to R_B and R_L [6]. An identical equation is also derived by Hinrichsen *et al.* [21] in a different manner. The fractal dimension is given by

$$D_s = \ln R_B / \ln R_L .$$

Applying this formula with $R_B = 5.3$ and $R_L = 2.7$ for our river pattern, we have $D_s = 1.66$ for $a = 1$ (see Table I for other cases). One of the authors (H.T.) also proposes another equation to calculate the fractal dimension of the branching geometry using β, the power-law exponent of the branch-size distribution [18]. The equation is

$$D_\beta = 1/(1-\beta) .$$

Substituting the power-law exponent of the drainage-basin area distribution from our simulation, $\beta = 0.42$, into this equation, we obtain the value of $D_\beta = 1.72$ in the case $a = 1$ (see Table I again for other cases).

These values of the fractal dimension of our river network are significantly smaller than 2, which is the fractal dimension of the space-filling geometries on the two-dimensional space. In our model, all of the lattice points in the system belong to the steady-state river pattern, and in the real system, if there is no stagnancy region of water, the rainwater falling on the land flows smoothly to join the river stream wherever the water falls in the system. So the fractal dimension of the river pattern must be 2 [5], and here a question arises as to why the above fractal dimensions of our river pattern are not 2.

In Fig. 11 we draw the branches of the steady-state river pattern having different drainage-basin areas created in the system of size 512×512. By this figure, we notice the fact that the total shape of the river branches is dependent on their drainage-basin area. More concretely, they have more elongated shape as they have larger drainage-basin area [22], so the self-similarity of the river pattern is broken and we have to treat the river patterns as self-affine objects. In general, the self-affine geometries

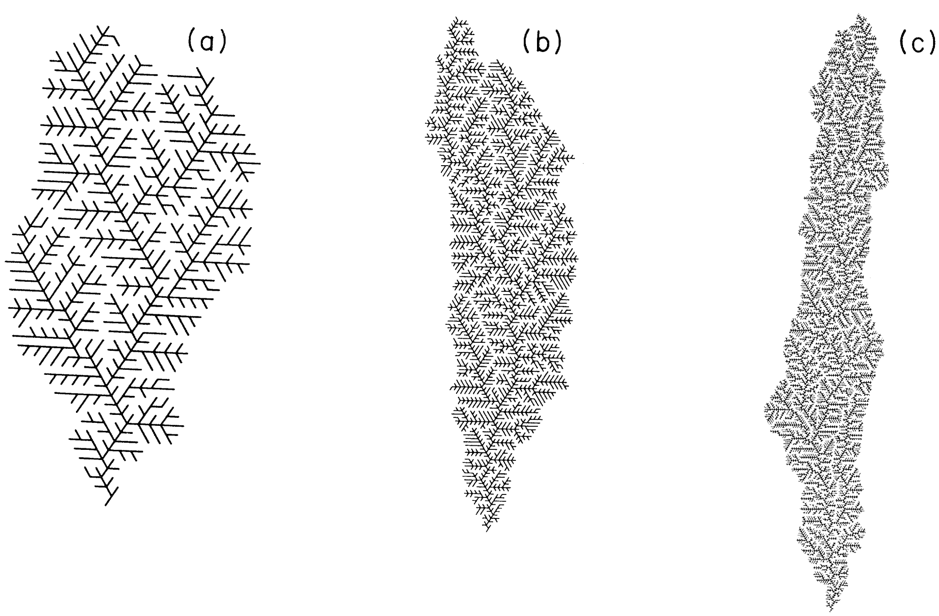

FIG. 11. The river network branches of different branch sizes from the steady-state river pattern. The drainage-basin shape is more elongated as they have larger basin area. (a) $n = 748$, (b) $n = 3257$, and (c) $n = 11\,020$.

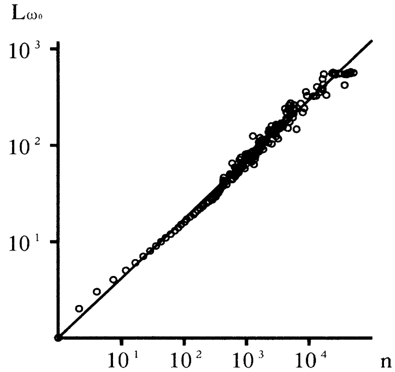

FIG. 12. The relation between drainage basin area n, and main stream length L_{ω_0} in log-log scale for the case $a=1$. The line shows the relation as $L \propto n^{0.62}$.

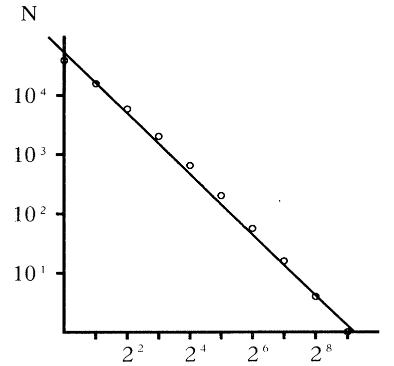

FIG. 13. The result of the box-counting method applied to the contour line. The number of the box N vs the size of the box r shown in log-log scale. The line used is 600.0 in height from the model of $a=1$ right after the river pattern becomes stationary.

cannot be characterized by a fractal dimension and as we observe the system by a larger scale, we get a smaller empirical value of fractal dimension [3]. So the fractal dimension smaller than 2 is probably caused by this self-affine property of the river networks.

The self-affine properties of drainage-basin shape imply the relationship between n, the drainage-basin area of a river, and L, its main stream length, which deviates from the usual relation $n \propto L^2$. Hack performed the detailed investigation of the real river networks and found the relation to be $L \propto n^{\alpha}$, $\alpha=0.6$ [22]. We check the validity of Hack's law in our model.

We again assign the stream order of our river patterns using Horton's method. An ω_0 order stream is followed by $\omega < \omega_0$ order streams making a branch, and this ω_0 order stream can be regarded as the main stream of the branch. In this way, we define the set of branches and plot their ω_0 order stream length L_{ω_0} versus the branch size n in log-log scale. As shown in Fig. 12, the points are on a straight line, and we estimate the value of $\alpha=0.60-0.64$ (Table I).

Mandelbrot interpreted Hack's law that an individual river stream should be a fractal of dimension $2\alpha=1.2$ assuming the self-similarity of the drainage-basin shape [1]. However, in our model, the fractal dimension of the main stream is confirmed to be very close to 1.0, so his speculation is not valid for our model. The relation between L_{ω_0} and n in Hack's law comes purely from the self-affine property of the river basin shape.

B. For the contour lines

As we can see from Fig. 2, the contour lines of land surface in our model seem to have some fractal properties. We check this intuition by the box-counting method. One of the results is shown in Fig. 13. The points are on a slightly convex line which roughly shows a power-law scaling property of the contour lines. But because of the convexity of the line, we cannot estimate the value of the fractal dimension accurately. Moreover, as we mentioned in Sec. VI A, the drainage-basin shape on the landform in our model has self-affinity. So the shape of the contour lines may also be influenced by this self-affinity, and then the fractal dimension cannot fully characterize the contour lines. In our previous paper [16] we made an attempt to estimate the fractal dimension of the contour lines, but it may be less meaningful.

VII. SUMMARY

One of the most important characteristics of the fractal geometries is their long-distance correlation. This characteristic is thought to be the result of the growth process under the influence of the surrounding structures. In other words, the mechanism or the "medium" which transmits the information about the surrounding structures to the local growth point is a crucial factor for the fractal growth system. We found that the water on the earth's surface plays the role of such a "medium." As shown in the above sections, our model automatically creates stable fractal geometries both in river patterns and earth's surfaces. This fact insists that the fractalities on the earth's relief can be created by water erosion as a fractal growth process, which is one of the most common factors of changing landscapes.

ACKNOWLEDGMENT

We would like to express our gratitude to Rikei Corporation for giving us the opportunity to use a massively parallel SIMD computer, MasPar MP-1204.

[1] B. B. Mandelbrot, *The Fractal Geometry of Nature* (Freeman, San Francisco, 1982).
[2] J. Feder, *Fractals* (Plenum, New York, 1988).
[3] T. Vicsek, *Fractal Growth Phenomena* (World Scientific, Singapore, 1989).
[4] H. Takayasu, *Fractals in the Physical Sciences* (Manchester University Press, Manchester, 1990).
[5] D. G. Tarboton, R. L. Bras, and I. Rodriguez-Iturbe, Wa-

ter Resour. Res. **24**, 1317 (1988).
[6] P. La Barbera and R. Rosso, Water Resour. Res. **25**, 735 (1989).
[7] T. A. Witten and L. M. Sander, Phys. Rev. Lett. **47**, 1400 (1981).
[8] L. Niemeyer, L. Pietronero, and H. Wiesmann, Phys. Rev. Lett. **52**, 1033 (1984).
[9] R. E. Horton, Bull. Geol. Soc. Am. **56**, 275 (1945).
[10] A. E. Scheidegger, Bull. I.A.S.H. **12**, (1), 15 (1967).
[11] L. B. Leopold and W. B. Langbein, U.S. Geol. Survey Prof. Pap. 500-A, 1 (1962).
[12] P. Meakin, J. Feder, and T. Jøssang, Physica A **176**, 409 (1991).
[13] G. Roth, F. Siccardi, and R. Rosso, Water Resour. Res. **25**, 319 (1989).
[14] G. Willgoose, R. L. Bras, and I. Rodriguez-Iturbe, Water Resour. Res. **27**, 1671 (1991).
[15] S. Kramer and M. Marder, Phys. Rev. Lett. **68**, 205 (1992).
[16] H. Takayasu and H. Inaoka, Phys. Rev. Lett. **68**, 966 (1992).
[17] P. Bak, C. Tang, and K. Wiesenfeld, Phys. Rev. Lett. **59**, 381 (1987); Phys. Rev. A **38**, 364 (1988).
[18] H. Takayasu, J. Phys. Soc. Jpn. **57**, 2585 (1988).
[19] A. E. Scheidegger, Water Resour. Res. **4**, 167 (1968).
[20] A. E. Scheidegger, Water Resour. Res. **4**, 1015 (1968).
[21] E. L. Hinrichsen, K. J. Måløy, J. Feder and T. Jøssang, J. Phys. A, **22**, L271 (1989).
[22] J. T. Hack, U.S. Geol. Surv. Prof. Pap. 294-B, 45 (1957).
[23] H. Takayasu, M. Takayasu, A. Provata, and G. Huber, J. Stat. Phys. **65**, 725 (1991).